Switching off the magnetic exchange coupling by quantum resonances

Ching-Hao Chang* and Tzay-Ming Hong†
Department of Physics, National Tsing Hua University, Hsinchu, Taiwan 300, Republic of China
(Received 3 May 2012; published 13 June 2012)

We clarify the role of quantum-well states in magnetic trilayer systems of the majority carrier in the ferromagnetic configuration and all carriers in the antiferromagnetic configuration. In addition to numerical and analytic calculations, heuristic pictures are provided to explain the effects of a capping layer and side-layer modulation in recent experiments. This immediately offers individual answers to two unexplained subtle findings in experiments and band-structure calculations. Furthermore, it allows a more flexible tuning of or even a turning off of the interlayer exchange coupling.

DOI: 10.1103/PhysRevB.85.214415 PACS number(s): 75.70.Ak, 72.25.Mk, 73.21.Fg, 75.47.De

I. INTRODUCTION

It was observed[1,2] more than 20 years ago that the interlayer exchange coupling (IEC) of ferromagnetic layers in a giant magnetoresistance (GMR) system oscillates between ferromagnetism and antiferromagnetism as a function of spacer width. This feature is ascribed to the Ruderman-Kittel-Kasuya-Yosida (RKKY) oscillation[3,4] and the formation of quantum-well states (QWSs) at Fermi surface.[5–7] These theories, based on the ideal system with infinite system widths, are successful at predicting the IEC periods. However, the theoretic values for their amplitudes always overestimate. Although the inevitable roughness on the interfaces was considered as the key factor to this disagreement in most cases,[8] the treatment of approximating the layer thickness as being semi-infinite should also play an important role.[9,10] The *ab initio* calculation[10] in Co/Cu/Co (100) and (010) has revealed that the coupling strength is very sensitive to the variation of side-layer (SL) thickness, which redistributes weightings among different RKKY modes. The physical origin in the (100) case was ascribed to the discrepancies between the Co density of state in the bulk and that in the thin layer, but in (010) the density of states is roughly the same and so it was put forward as a subtle challenge.

In addition, the experimentalists[11–13] found that the coupling strength displayed an oscillatory feature as the SL thickness was varied. It was discovered recently that, with an insulating capping layer and by varying SL thickness, the scattering properties in the SL edge became tunable.[11] In contrast to the usage of a metallic cap, the oscillation amplitude got stronger and a novel RKKY period was deduced.[11] The quantum resonance, which is altered by the scattering paths reflected between the bottom of capping layer and the top of spacer, would be crucial to explain (1) the origin of disagreements for the noble-metal spacer[4] and (2) the creation of a new IEC period observed in recent experiments.[11] Another motivation for studying the finite-size effect for IEC is that it may enable us to either enhance or shut off entirely the IEC by proper nanoconfigurations. A known example of such applications is the diluted magnetic semiconductors (DMSs), where a room-temperature ferromagnetic phase has been obtained by replacing the magnetic impurities with the self-organized nanocolumns.[14] The quantum resonance in these nanocolumns, which is realized at properly chosen sizes, enhances the RKKY coupling between clusters and achieves a higher transition temperature for the DMSs.[15]

II. CALCULATION

To realize how the boundaries with the capping layer and substrate for finite ferromagnetic layers affect the IEC, we start with the GMR consisting of a noble-metal spacer, in which the minority carriers are confined in the spacer and their quantum resonance near the Fermi surface will determine the positions of peaks in the IEC oscillation.[6,16] The Fe/Ag/Fe (001) trilayer is calculated within the single-electron picture with different energy barriers in respective layers.[17] Besides, we assume that both the substrate and the capping layer play the roles of infinite potential barriers to simulate the recent experimental setup.[11] The exchange coupling is defined as the relative energy difference $J = (\Delta E_{\mathrm{AFM}} - \Delta E_{\mathrm{FM}})/A$, with A being the interface area, FM being ferromagnetic, and AFM being antiferromagnetic. The ΔE_{FM} (ΔE_{AFM}) denotes the system energy of normal order for the FM (AFM) configuration. For the case of FM, this energy is calculated by

$$\Delta E_{\mathrm{FM}} = A E_F \sum_{\sigma=\uparrow,\downarrow} \sum_{n=0}^{\infty} \int d^2 k_{\parallel}/4\pi^2 \times \frac{E(\sigma,n)/E_F + k_{\parallel}^2/k_F^2 - 1}{\exp\left[\left(E(\sigma,n)/E_F + k_{\parallel}^2/k_F^2 - 1\right)\frac{E_F}{k_B T}\right] + 1}, \quad (1)$$

where $E(\sigma,n)$ is the energy of nth bound state for carriers with spin orientation σ in the confined trilayer, $k_{\parallel}$ is the transverse wave vector, and T is the temperature. Note that E_F/k_F is assigned to denote the Fermi energy/momentum for the spacer and q_F is the Fermi momentum for the majority carrier in SL from now on.

To describe the Fe/Ag/Fe (001) system in the interface zone center at $k_B T = 10^{-4}$ eV, Eq. (1) and the coupling strength J can be estimated by setting $E_F = 4$eV and $1/k_F = 4$ Å, and the potential barrier for the majority/minority carrier in SL is 5/3 eV.[17,18] Figure 1 is the schematic illustration for the estimation of $\Delta E_{\mathrm{FM/AFM}}$ and one can refer to Eqs. (1)–(6) in Ref. 19 for details on the calculations. In Fig. 2, the spacer width D is fixed while J is plotted as a function of SL thickness, D_{Fe}. Consistent with the experimental findings, the oscillation period is dominated by and equals half of the Fermi wavelength of the majority carrier in the FM SL. Similar to the conventional RKKY oscillation, J also displays the power-law decay and approaches the result of a semi-infinite system as $D_{\mathrm{Fe}} \to \infty$. In Fig. 3, we study the effect of D on J while

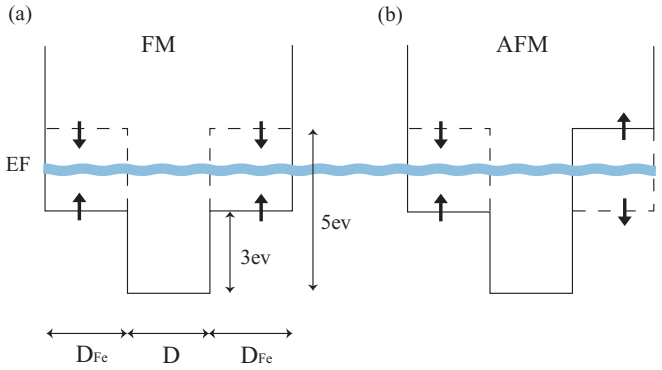

FIG. 1. (Color online) A plot of the spin-dependent effective potential for (a) the FM configuration and (b) the AFM configuration of the Fe/Ag/Fe (001) trilayer in the interface zone center. The blue thick line denotes the Fermi surface, and solid (dotted) lines are the barriers for the electrons with majority (minority) spin.

the SL width is fixed at the values which correspond to one of the peaks and troughs, respectively, in Fig. 2. Although the extreme values of J occur at roughly the same spacer widths, which is consistent with experiments,[7,20] their amplitudes are sensitive to the specific choice of SL thickness, with a possible enhancement of doubling the semi-infinite value at $k_F D > 14$. Overall, the thicker the D, the larger is the enhancement.

III. ANALYSIS AND INTERPRETATION

In the semi-infinite case which contains a noble-metal spacer, Oretega *et al.*[5,6] noticed that the minority state or equivalently the QWS could be generated periodically as a function of spacer width, while the unbound majority state is nearly unaffected. The extreme values of J appear as the minority carrier from QWS. However, all realistic systems are of finite size, especially when in nanoscale the confinement and formation of QWSs in FM/AFM configurations come from not just the minority but all carriers. One interesting consequence is that the amplitude of J becomes tunable by adjusting the SL

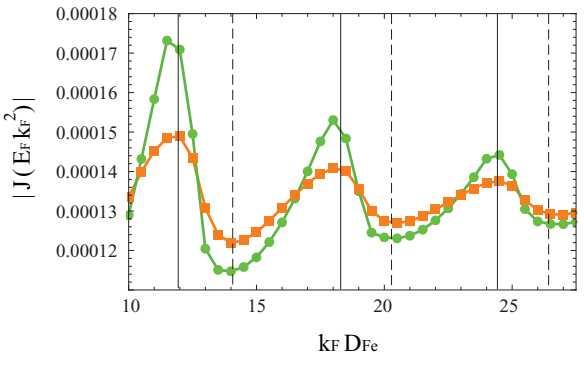

FIG. 2. (Color online) Coupling energies for Fe/Ag/Fe (001) trilayer with a fixing $D = 5/k_F$ are estimated for different SL widths. Both SLs are of equal finite width for the circle points. In contrast, the square points represents some experimental conditions where one of the SL is semi-infinite, which we mimic by setting $D = 200/k_F$. The solid (dashed) vertical lines are the theoretic prediction of where the peak (trough) values will occur, on which more discussion follows in Fig. 5.

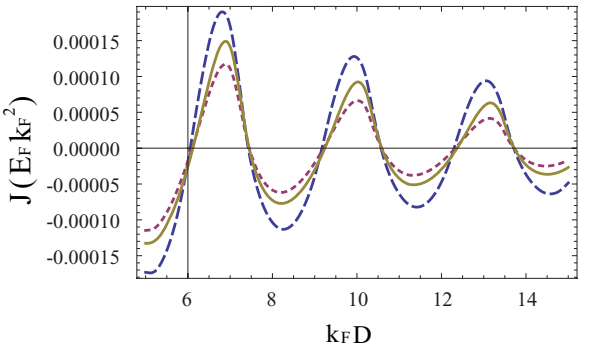

FIG. 3. (Color online) Coupling energies plotted as a function of D for Fe/Ag/Fe (001). The solid line denotes the case where both SLs are set at $k_F D_{\mathrm{Fe}} = 200$ to mimic the semi-infinite system. The dashed (dotted) lines are for finite systems where $k_F D_{\mathrm{Fe}} = 11.5$ (14) corresponds to the first peak (trough) of the solid line in Fig. 2.

thickness, as shown in Fig. 3. Although being unable to derive this, Refs. 5 and 6 correctly predicted the special spacer widths that could render the extreme values. The schematic diagrams in Fig. 4 provide heuristic pictures for understanding how SL thickness alters the relative positions of quantum resonances for different carriers and makes such a manipulation possible. The energy barrier height in the SL is set to be zero (infinity) for the majority (minority) carrier for convenience without loss of generality.

The SL thickness in Fig. 4(a) allows constructive interferences for the majority carrier in the FM configuuration (see middle plot) and for both carriers in the AFM (bottom

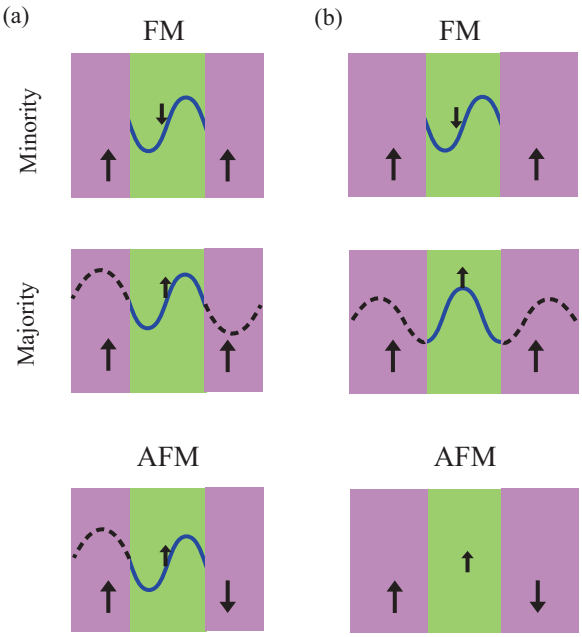

FIG. 4. (Color online) Schematic diagrams that exemplify (a) the coherent case, which characterizes the simultaneous appearance of quantum resonances for carriers in the FM and AFM configurations, and (b) the incoherent case, by adding a quarter Fermi wavelength to both SL thicknesses. All carriers in the AFM no longer sustain QWSs due to the violation of boundary conditions. The big (small) arrow denotes the moment (spin) orientation of the SL (carrier).

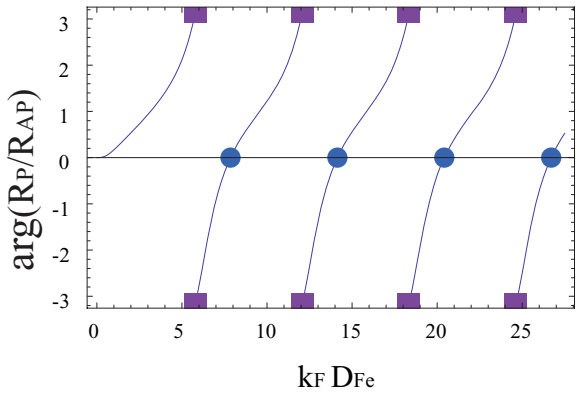

FIG. 5. (Color online) The argument of R_P/R_{AP} is plotted as a function of SL thickness. Since $|R_P| = |R_{AP}| = 1$, the zero arguments (in circles) denote the case of $R_P = R_{AP}$, which allows coherent resonances. While $\pm\pi$ arguments (squares) are for $R_P = -R_{AP}$, which induces incoherent resonances.

plot) configuration. Since these resonances are absent in the semi-infinite case, they enhance the system energy of both configurations by an amount that is roughly double in the AFM than in the FM. When taking their difference, J turns out to be weaker. In Fig. 4(b), we add a quarter Fermi wavelength to both SL thicknesses. The resonance is ruined in the AFM configuration, but is kept alive in the FM. This results in an enhanced J as compared to the semi-infinite case. Irrespective to whether the capping layer and substrate are metallic or insulating, the effective reflection coefficient at both edges of the spacer can be calculated after the inclusion of additional scattering paths that are reflected by them,

$$R_P(r_c, D_{\mathrm{Fe}}) = \frac{r_P + r_c e^{2iq_F D_{\mathrm{Fe}}}}{1 + r_P r_c e^{2iq_F D_{\mathrm{Fe}}}}, \tag{2}$$

where r_P and r_c denote the reflection coefficient for the majority carrier reflected by SL and the capping layer, respectively. The coefficient R_{AP} for the minority carrier obey a similar equation as Eq. (2), except the wave vector q_F in SL becomes complex. The condition for the formation of a QWS is $R^2_{P/AP} e^{2ik_F D} = 1$ for majority/minority carrier in the FM configuration, in contrast to $R_P R_{AP} e^{2ik_F D} = 1$ for both carriers in the AFM configuration. These three relations allow us to deduce the necessary condition for the coherent case as $R_P = R_{AP}$ as opposed to $R_P = -R_{AP}$ for the incoherent one. The connection between the hugely tunable J and our heuristic picture of an incoherent (coherent) appearance of QWS is confirmed by comparing Fig. 5 with the SL thicknesses that correspond to an enhancement (reduction) of J in Fig. 2.

In order to study the enhancement in more detail, we start from the asymptotic form of IEC within the free electron model and assume that SLs are made of the same material:[3]

$$\lim_{k_F D \gg 1} J \approx \frac{-E_F k_F^2}{8\pi^2 (k_F D)^2} \mathrm{Im}[(r_P - r_{AP})^2 e^{2ik_F D}]. \tag{3}$$

By expanding $(r_P - r_{AP})^2$, the quantum interferences for r^2_{AP}, r^2_P, and $-2r_{AP}r_P$ terms are each characterized in top, middle, and bottom plots in Fig. 4. Quantitatively, $|r_{AP}| \approx 1$ is much bigger than $|r_P|$ in the semi-infinite case, as opposed to being exactly equal in the cases of finite and sustaining QWSs. This

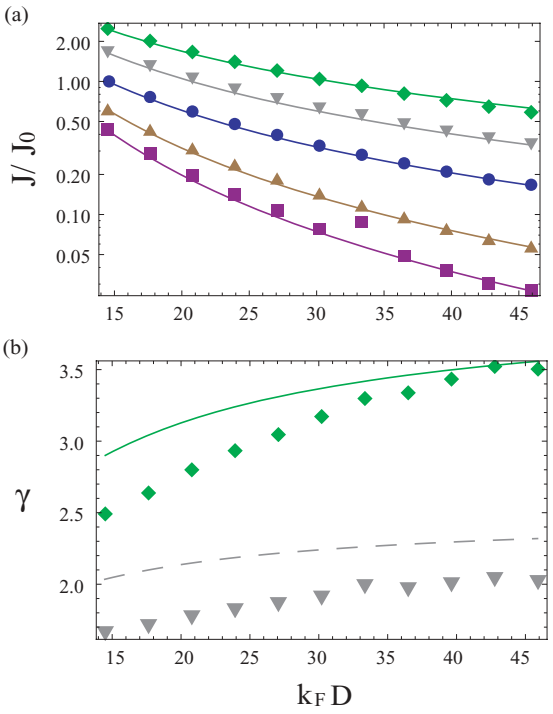

FIG. 6. (Color online) (a) The peak values of coupling strength for Fe/Ag/Fe (001) with different arrangements of SL thickness: semi-infinite (circles), of the same thickness $k_F D_{\mathrm{Fe}} = 5.79$ (7.85) [diamonds (squares)], and with one obeying $k_F D_{\mathrm{Fe}} = 5.79$ (7.85), while the other is semi-infinite [inverted triangles (triangles)]. The unit J_0 is the coupling strength for the semi-infinite case with $k_F D = 14.5$. All five lines are fitted by a power-law decay with exponent $-1.18, -1.38, -1.56, -2.06$, and -2.41 from top to bottom. (b) Same plot for the enhancement ratio with the same thickness $k_F D_{\mathrm{Fe}} = 5.79$ for both SLs (diamonds) and with one SL set to be semi-infinite (inverted triangles). The solid and dashed lines are plotted from Eqs. (4) and (5), respectively.

implies that the maximum enhancement from the incoherent resonance $R_P = -R_{AP}$ could reach as high as four times in the semi-infinite case. This prediction is verified in Fig. 6(a). In Fig. 3, it was observed that the enhancement ratio got bigger as D increased. This can also be explained by examining the denominator of Eq. (3). For finite SL, the contribution from the majority carrier in FM needs to be modified to $R^2_P/(k_F D + 2q_F D_{\mathrm{Fe}})^2$, while that from the minority remains the same. In contrast, the contribution from both carriers in the AFM configuration is changed to $-R_{AP}R_P/(k_F D + q_F D_{\mathrm{Fe}})^2$.

Let us now concentrate on the incoherent case. When $D \gg 2(q_F/k_F)D_{\mathrm{Fe}}$, the contribution from all carriers becomes roughly $R^2_{AP}/(k_F D)^2$ and equals that of the minority. On the other hand, it is much smaller when $D \ll 2(q_F/k_F)D_{\mathrm{Fe}}$. So one should adopt a thick spacer in order to obtain a large enhancement ratio, $J(D)/J(D \ll 2(q_F/k_F)D_{\mathrm{Fe}})$, which depends on

$$\gamma \approx 1 + \left(\frac{k_F D}{k_F D + 2q_F D_{\mathrm{Fe}}}\right)^2 + 2\left(\frac{k_F D}{k_F D + q_F D_{\mathrm{Fe}}}\right)^2. \tag{4}$$

In the above case, all carriers are totally reflected at both edges and satisfy $R_P = -R_{AP}$. However, when the substrate is semi-infinite or the top of the GMR is either connected to a

contact or capped by a metal layer, this side of the SL should be treated as being semi-infinite. It will adopt the coefficients r_P and r_{AP} for the semi-infinite case, and the path factor for additional resonances equals $k_F D + q_F D_{\mathrm{Fe}}$. As a result, Eq. (4) is modified to

$$\gamma' \approx 1 + |r_{ap} + 2r_p| \left(\frac{k_F D}{k_F D + q_F D_{\mathrm{Fe}}} \right)^2. \tag{5}$$

It is obvious that Eq. (5) is always less than Eq. (4) when D is large, which explains why the amplitude of the square line in Fig. 2 is smaller than that of the circle one. Both Eq. (4) and Eq. (5) are consistent quantitatively with the numerical results in Fig. 6(b). The nearly constant shift between Eq. (5) and our calculation is due to the fact that the SL thickness we chose only generates approximate incoherent resonance in the system with one semi-infinite SL.

IV. DISCUSSION

A final implication is that we may have solved the puzzle put forward by Halley *et al*. in Ref. 11. By capping Fe/Cr/Fe, they managed to observe a novel period for $J(D)$, long predicted and sought after by the band-structure calculations.[18] As was argued by the authors of Ref. 11, we provide a concrete physical process to explain how this additional confinement can lead to revival or suppression of the contribution to IEC from a particular channel via modifications of the reflection coefficient at Fe/Cr. Equations (4) and (5) have concentrated on the enhancement effect. Let us now derive in more detail how the suppression comes about. Mainly, one needs to create the coherent conditions mentioned in Fig. 4(a). The coupling strength of the square line, which represents the coherent case, has the highest decaying rate than the other four lines in Fig. 6(a). Its magnitude can be about one and two orders smaller than the circle (for the semi-infinite case) and diamond lines (incoherent case) at the largest D value in the figure, respectively. This weak coupling that results from this nonconventional RKKY oscillation, which is generated by $R_P = R_{AP}$, can be estimated by converting the plus sign for the third term in Eq. (4) to minus:

$$J\left(D \gg 2\frac{q_F}{k_F} D_{\mathrm{Fe}} \right) \approx -\frac{E_F D_{Fe}^2}{4\pi^2} \frac{\sin(2k_F D + \phi)}{D^4}. \tag{6}$$

The reason why this decaying power is higher than those obtained numerically in Fig. 6(a) is that the asymptotic form in Eq. (3), on which Eq. (6) is based, is only an approximation and the higher-order terms are not rigorously negligible for trilayers with a noble-metal spacer.[21]

Although there are many factors that may affect the RKKY oscillation in the real Fe/Cr/Fe sample, our calculation confirms that the resonances in both SLs have the capability to drastically change the IEC strength. Another noticeable property is that GMR has multiperiod RKKY oscillations, which is common in most experiments, and these modes can be separately tuned by varying the SL thickness, that is, changing their resonant conditions. Their relative weightings are also affected by the SL and capping layer thickness. We are confident that the predictions and explanations above for Fe/Ag/Fe can be equally applied to Co/Cu/Co. Nevertheless, a quantitative match will require a more detailed *ab initio* calculation than the pioneering work by Nordström *et al*.[10] For instance, they calculated the density of states for a single Co SL and showed that different thicknesses could lead to redistribution of RKKY modes. However, they could not locate the origin of this dependence in the (010) crystal direction since the density of states they obtained was not sensitive to varying SL thickness. Based on our predictions, we propose to redo the calculations for the whole trilayer, namely, include the spacer and both SLs.

V. CONCLUSION

In conclusion, we find that the strength of IEC for GMR with a capping layer can be modulated by as much as two orders of magnitude through careful arrangement of SL thickness. This is made possible by creating coherent (to suppress IEC) or incoherent (to enhance) QWSs in the FM and AFM configurations. This immediately offers individual answers to two outstanding puzzles in experiments[11] and band-structure calculations.[10] We provided heuristic physical pictures and both numerical and analytic calculations to support our conclusions. Moreover, the discrepancy between theoretic predictions for IEC strength of trilayers and experimental findings, which was ascribed to the interface roughness,[4] also receives an alternative explanation. Our mechanism carries another potential merit in enabling experimentalists to eliminate the intergranular exchange coupling in the hard disk drives[22] and other future spintronic devices.

ACKNOWLEDGMENTS

We thank K. Lenz, M. Körner, J. McCord, C. R. Chang, M. T. Lin, C. M. Wei, C. H. Lai, and C. C. Chi for valuable comments and discussions. The authors acknowledge support by the NSC in Taiwan and DAAD in Germany.

*cutygo@gmail.com
†ming@phys.nthu.edu.tw

[1] C. F. Majkrzak, J. W. Cable, J. Kwo, M. Hong, D. B. McWhan, Y. Yafet, J. V. Waszczak, and C. Vettier, Phys. Rev. Lett. **56**, 2700 (1986).
[2] P. Grünberg, R. Schreiber, Y. Pang, M. B. Brodsky, and H. Sowers, Phys. Rev. Lett. **57**, 2442 (1986).
[3] P. Bruno, Phys. Rev. B **52**, 411 (1995).
[4] M. D. Stiles, J. Magn. Magn. Mater. **200**, 322 (1999).
[5] J. E. Ortega and F. J. Himpsel, Phys. Rev. Lett. **69**, 844 (1992).
[6] J. E. Ortega, F. J. Himpsel, G. J. Mankey, and R. F. Willis, Phys. Rev. B **47**, 1540 (1993).
[7] Z. Q. Qiu and N. V. Smith, J. Phys.: Condens. Matter **14**, 169 (2002).
[8] C. H. Chang and T. M. Hong, Phys. Rev. B **79**, 054415 (2009); **82**, 094415 (2010).
[9] P. Bruno, Europhys. Lett. **23**, 615 (1993).

[10]L. Nordström, P. Lang, R. Zeller, and P. H. Dederichs, Phys. Rev. B **50**, 13058 (1994).
[11]D. Halley, O. Bengone, S. Boukari, and W. Weber, Phys. Rev. Lett. **102**, 027201 (2009).
[12]S. N. Okuno and K. Inomata, Phys. Rev. Lett. **72**, 1553 (1994).
[13]K. Inomata, S. N. Okuno, Y. Saito, and K. Yusu, J. Magn. Magn. Mater. **156**, 219 (1996).
[14]M. Jamet, A. Barski, T. Devillers, V. Poydenot, R. Dujardin, P. Bayle-Guillemaud, J. Rothman, E. Bellet-Amalric, A. Marty, J. Cibert, R. Mattana, and S. Tatarenko, Nat. Mater. **5**, 653 (2006).
[15]C. H. Chang and T. M. Hong, Appl. Phys. Lett. **93**, 212106 (2008).
[16]F. J. Himpsel, J. E. Ortega, G. J. Mankey, and R. F. Willis, Adv. Phys. **47**, 511 (1998).
[17]N. V. Smith, N. B. Brookes, Y. Chang, and P. D. Johnson, Phys. Rev. B **49**, 332 (1994).
[18]M. D. Stiles, Phys. Rev. B **48**, 7238 (1993); **54**, 14679 (1996).
[19]Z. N. Hu, J. Z. Wang, and B. Z. Li, J. Phys.: Condens. Matter **13**, 215 (2001).
[20]Z. Q. Qiu, J. Pearson, and S. D. Bader, Phys. Rev. B **46**, 8659 (1992).
[21]A. T. Costa Jr., J. d'Albuquerque e Castro, M. S. Ferreira, and R. B. Muniz, Phys. Rev. B **60**, 11894 (1999).
[22]J.-G. Zhu, Mater. Today **6**, 22 (2003).